



Research paper

Compression behaviour of BFRP bars

Marek Urbański¹, Kostiantyn Protchenko²

Abstract: The durability of building structures reinforced by steel is one of the main concerns in civil engineering. Currently, research in the field is focused on the possibility of replacing steel with relatively corrosion-resistant reinforcement, such as BFRP (Basalt Fiber Reinforced Polymers) bars. The behaviour of BFRP bars during compression has not yet been determined. The experimental results pertaining to BFRP bars subjected to compression were presented and discussed in the paper. The research program involved the preparation of 45 BFRP samples with varying unbraced length and nominal diameter of 8 mm that were subjected to compression. For samples with the unbraced length of up to 85 mm, the destruction was caused by crushing. The bars with the unbraced length greater than 120 mm were destroyed as a result of global buckling of the bar and subsequent fiber kinking. Based on the relationship between the buckling load strength – unbraced length, the optimal unbraced length of BFRP bar was determined, for which buckling load strength reaches its maximum value. The buckling load strength decreased, as the unbraced length increased. The values of modulus of elasticity under compression for variable unbraced lengths were slightly different for the samples, and were similar to the modulus of elasticity obtained at the tensile testing. The relationship between the buckling load strength and the unbraced length of BFRP bars was determined. This may contribute to the optimization of the transverse reinforcement spacing in compressed elements and to the development of standard provisions in the area of elements reinforced with FRP bars being subjected to compression.

Keywords: BFRP reinforcement, buckling, compression properties, compression, crushing, SEM analysis

¹PhD., Eng., Warsaw University of Technology, Faculty of Civil Engineering, Al. Armii Ludowej 16, 00-637 Warsaw, Poland, e-mail: m.urbanski@il.pw.edu.pl, ORCID: 0000-0002-3568-6888

²MSc., Eng., Warsaw University of Technology, Faculty of Civil Engineering, Al. Armii Ludowej 16, 00-637 Warsaw, Poland, e-mail: k.protchenko@il.pw.edu.pl, ORCID: 0000-0003-1357-2174

1. Introduction

For the last few decades the use of Fiber Reinforced Polymers (FRP) composites for concrete structures has experienced explosive growth. A major reason of its implementation lies in the unique characteristics of these materials and their appropriate use for considered design purpose. Numerous investigations have shown that FRP composites are effective materials for use in concrete members [1–3].

The use of FRP composites in strengthening of concrete structures has become an efficient alternative to some of the existing traditional methods due to their features in terms of strength, lightness, corrosion resistance and ease of application. The strengthening techniques of Near-Surface Mounted (NSM) or Externally Bounded (EB) reinforcements can be also very attractive due to their quick installation and low labour costs [4–6].

The application of FRP bars as internal reinforcement in concrete members has many advantages as opposed to structural members reinforced with steel bars [7]. Durability, strength and stability are the main criteria when selecting a material in the design of concrete structures with internal FRP reinforcement [8–10].

The standards for the design of reinforced concrete (RC) structures, such as Eurocode 2 [11] or ACI318-19 [12] etc., represent recommendations for the design with a conventional steel reinforcement. However, the available data from existing standards on FRP reinforcement, ACI440.1R-06 [13], ACI 440.1R-15 [14] and CNR- DT 203 [15] regarding compressive strength of FRP bars are scarce. In accordance with Canadian standard CSA S806-12 the values for compressive strength and stiffness of FRP bars should be assumed as zero [16].

The value of tensile strength of the reinforcement depends on its physical and mechanical properties obtained during testing, such as yielding strength, modulus of elasticity and others. However, the compressive strength of concrete element is determined mainly by strains at concrete, when its ultimate compressive strength is achieved. The limit strains of concrete depend on its class, composition and duration of load. As the concrete class increases, the limit strains decrease. At the same time, the limit strains can increase due to load duration. The transverse reinforcement in the form of stirrups for the compression element effectively stops lateral deformation, and thus its load capacity can be significantly increased. On the other hand, when compressed, BFRP elastic reinforcing bars tend to lose stability (due to bulging) long before the strength limit is exhausted and the protective concrete cover is broken. This issue can cause premature structural failure. To prevent this dangerous phenomenon, it is necessary to use the appropriate spacing for transverse reinforcement. Therefore, the effect of unbraced free length on the buckling load strength of BFRP bars plays a significant role in the design of RC structures.

1.1. Properties of BFRP bar

Basalt-Fiber Reinforced Polymers (BFRP) bars have several advantages over traditional steel reinforcement. These include, among others, low weight, high tensile strength, corrosion resistance and transparency to magnetic fields. Compared to steel bars, BFRP bars are

characterized by a relatively low modulus of tensile strength [17]. However, compared to the most common Glass Fiber Reinforced Polymer (GFRP) bars, BFRP bars show significantly greater resistance to alkali and acids [18]. In addition, the BFRP bars are characterized by high resistance to elevated temperatures. Tensile strength tests of BFRP bars after 90 minutes at 300°C confirmed a much smaller reduction in strength properties (10%) compared to GFRP bars (75%) [19].

Processing of BFRP bars is analogous to the manufacturing of other FRP types, a certain amount of basalt rovings is embedded in epoxy resin. Basalt fibres are made from an inert natural rock; no chemical additives are used in the production. Basalt fibers do not react toxically with an air, water or other chemicals that may be hazardous to humans or may pollute the environment. In addition, basalt fibers are not carcinogenic [20]. During recycling, the fibers transform into a black powder, that can be easily removed from the combustion chamber and can be used as a filler for various applications.

1.2. Purpose and scope of research

The aim of the study, according to the proprietary compression test method, was to determine the scope of application of the BFRP reinforcement and its standardization in compressed RC elements. The scope of the research included samples of BFRP rods of various non-anchored lengths. This made it possible to determine a rational spacing of the transverse reinforcement in the compressed RC elements in order to effectively resist lateral deformations. Moreover, the tests allowed for the optimization of the compressive strength of the BFRP reinforcement on the basis of the determined strength – free length correlation of a bar.

1.3. Destruction mechanism of FRP bar

During the application of compressive loading, the matrix in the FRP composite material performs an important function, which is to ensure transverse stiffening and stabilization of the fibers due to the longitudinal compressive load. The modulus of elasticity of matrix is relatively low compared to the modulus of elasticity of fibres, however, the failure caused by longitudinal compression is often initiated by local fiber buckling. Depending on whether the matrix behaves elastically or exhibits plastic deformations, two different local buckling types can be observed: elastic micro-buckling and fibers kinking [21].

Extensional micro-buckling mode occurs when a small volume fraction of fibres ($V_f < 0.2$) is applied, and causes tensile strains in the matrix due to the external buckling of the fibers. Shear mode of micro-buckling occurs at high volume fractions of fibers causing shear strains in the matrix due to buckling inside the fibers. Due to the fact that in most of FRP composites, the volume fraction of fibers exceeds 60%, the shear mode of failure is more common than the extensional mode.

The second buckling type is the fiber kinking, which occurs in strongly localized areas, where the fibers are initially slightly shifted relating to the direction of the compressive load. Fiber bundles in these areas can become rotated relating to their initial configuration,

creating bands of refraction, and the surrounding matrix undergoes high shear deformation. Experiments carried out on glass and carbon fiber reinforced composites show the presence of fiber breakage at the ends of kinking bands [22]. However, whether fiber breakage precedes or follows the formation of a flexural band has not been experimentally verified [23].

As a result of the longitudinal compressive load of FRP composites, in addition to micro-buckling and kinking of fibers, many other methods of destruction were also observed. These include: shear damage, destruction due to crushing or bending reinforcement, longitudinal splitting in the matrix due to the Poisson effect, plasticizing of the matrix, delamination between strands of fibers and splitting of fibers and others [24].

2. Research program

2.1. BFRP bar compression test procedure

BFRP bars were tested from the same batch to ensure uniform material properties. BFRP bars of 9 different free lengths of 5 pieces were tested. The term “free length – (L'_f)” means the length of the bar between the sample anchors. The differentiation of the free lengths of the bar reflects the behavior of the composite longitudinal reinforcement limited by the spacing of the stirrups. The specimens were made of BFRP bars with an equivalent diameter $d_b = 8.32$ mm. The total length of the samples $L = L_a + L_f + L_a$ consists of two anchorages lengths and free, unbraced length of the BFRP bar. The average value of the equivalent bar diameter was determined in accordance with procedure B1 of the ACI 440.3R standard [29]. The parameter L_a is the length of the anchoring of the bar at both its ends and it was equal to the longitudinal dimension. Since the unbraced length of the longitudinal reinforcement bars may differ in the compressed elements depending on the spacing of the spiral or stirrups, it is necessary to establish the relationship between the buckling load strength and the unbraced length of the bars. The value of the measuring length (free, unbraced length of the sample) was multiplied by the diameter of the tested bars, i.e. $L_f = n \cdot d_b$. The tests were carried out for the next nine values of $n = 4, 6, 10, 12, 14, 16, 20, 22, 26$ (five samples for successive diameters). The steel sleeves had a length of 120 mm and an outer diameter of 40 mm. The bars were centrally fixed in the sleeves after degreasing them, using a special adhesive with a hardener. At the first step, the bar was anchored in one of the sleeves and then after the connection was cured, the other end of the sample was anchored (Fig. 1a). Due to the provided adhesion between the anchorage and the bar, its movement is prevented.

Designed anchorages in the sleeves are designed to absorb the compressive force through the side surface of the sample. The anchorages prevent to degradation of the bar ends, and the bar itself does not move during the testing, which may result in premature buckling. The coaxial arrangement of the bars was ensured by positioning lugs installed at both ends of the anchorage. In addition, there is no need to check the perpendicularity of the bar ends surface to its longitudinal axis. The strain gauges were attached with an

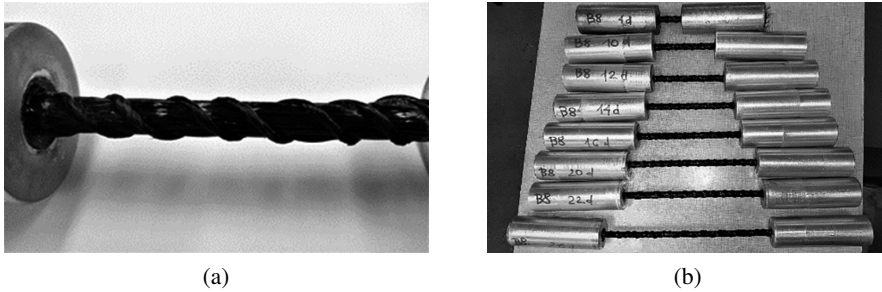


Fig. 1. Specimen preparation: (a) anchoring the bar in steel sleeves, (b) anchoring the bar specimens in steel sleeves at both sides

adhesive material by previously adjusting the side surface of the bar in the middle of the length of the unbraced bar. The data was recorded by two strain gauges (Techno-Mechanik, model RL20) with the length of 30 mm, a measuring length of 20 mm. Fig. 2a shows the test setup of the sample and Fig. 2b shows the destruction of BFRP bar, immediately after the testing.



Fig. 2. (a) Device for testing the BFRP reinforcing bars, (b) BFRP sample with free unbraced length of $26d_b$ damaged due to buckling

2.2. The buckling load strength of BFRP bars

The buckling load strength of BFRP bar specimens was determined according to the relationship:

$$(2.1) \quad f_{f,c} = F_u / A_{f,\min}$$

where: F_u is the maximum force registered during the test; $A_{f,\min}$ is the minimum bar diameter measured immediately before installing the strain gauges on the surface of the bar being tested.

The influence of shear load and radial tensile load occurring in the intermediate zone from the test sleeve to the bar on the sample destruction process is not taken into account.

To carry out the testing on longitudinal compression of BFRP bars, it was needed to make several assumptions. In order to obtain consistent and repeatable results, the gradual increasing of the load was required. The compression ratio was generally set at about 100 MPa/min for compression testing, so that the destruction of samples occurred within approximately 6 minutes. The specimens were tested by a 200 kN self-reaction WPM ZD20 machine with a displacement control approach using a testing rate of 0.5 mm/min. The rate of outcomes readings was set as 5 readouts per second. The axial strains, loads and stroke displacements were recorded.

2.3. The method of determining the deformation modulus

Determination of the modulus of elasticity under compression was carried out in accordance with the provisions of the ACI 440.3R-15 standard [29]. Since the behaviour of the samples, as a result of loading and deformation, shows the linearity of the modulus of elasticity, $E_{f,c}$, it was determined by dividing the difference of stresses by the difference of strains for the values of 0.5 and 0.2 of the breaking force. Modulus of elasticity, determined in this way, is the tangent of the secant inclination passing through the two mentioned points.

2.4. The method of determining the compressive strength with buckling

For slender bars, the parameter of the unbraced length is more significant than the dimensions of the cross-sections, since the loss of stability occurs in the elastic range of work of the material. For elastic buckling, the critical force value can be determined from the formula according to Euler's solution:

$$(2.2) \quad f_{fu,c} = \frac{\pi^2 \cdot E_{f,c}}{\left(\frac{k \cdot L_f}{r}\right)^2}$$

where: $f_{fu,c}$ – ultimate compressive stress; L_f – unbraced length; $E_{f,c}$ – compression modulus of elasticity; k – effective length coefficient for buckling; and r – radius of inertia of the BFRP bar.

3. Test results and discussion

3.1. SEM analysis of FRP bars

Qualitative and semi-quantitative elemental composition analyses using the secondary X-ray energy dispersion spectrometer (EDS) provided by the authors defines relevant information on the composition of BFRP bars. Based on the conducted research, it was

found that the dominant compounds in basalt fibers are SiO_2 and Al_2O_3 , which are also present in glass fibers. In addition, basalt fibers contain chemical compounds such as: MgO , Na_2O , K_2O , CaO , TiO_2 , Fe_2O_3 and FeO (Fig. 3).

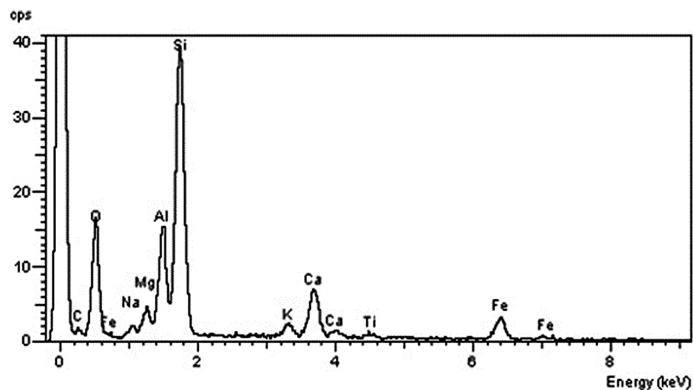


Fig. 3. Spectrographic analysis of BFRP bar basalt fibers

Chemical composition of basalt fibres can significantly influence their physical and mechanical characteristics and, in turn, properties of the bars. For example, the content of iron compounds affects the properties of basalt fibers, such as density (2.73 g/cm^3 for basalt fibers, compared to 2.54 g/cm^3 for type E glass fibers), colour (from brown to matt green, depending on FeO content), thermal conductivity and temperature stability [25, 26].

In addition, BFRP bars were tested using the Backscattered Electrons (BSE) method, which provided important information on the diversity of sample composition. In BSE images, the contrast is the result of the difference in the average atomic number between individual points of the sample. Darker areas in Fig. 4 indicate the position of the epoxy matrix, while lighter areas of circular shape are related to individual basalt fibers.

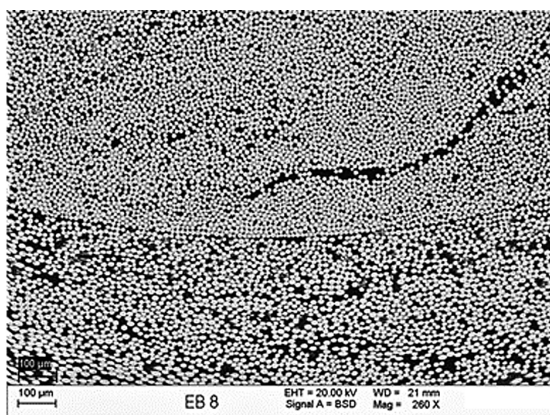


Fig. 4. BFRP bar (260× magnification), individual basalt roving fibers represented as bright points; the darker area is the epoxy matrix

Consecutively, the diversity of the chemical composition of basalt rocks significantly affects the differences in tensile strength and modulus of elasticity from 2000 to 4000 MPa and from 80 to 90 GPa, respectively [18, 27, 28]. KV42 basalt rovings, of which the tested BFRP bars were made, show significantly lower distribution of tensile strength and modulus of elasticity from 2900 to 3200 MPa and 87 ± 2 GPa [20]. This can be caused due to the scattering in the basalt fiber diameters, which can be observed in Fig. 5a. In the central part, a very bright area is visible, which indicates the content of FeO responsible for the olive-brown coloration of basalt fibers.

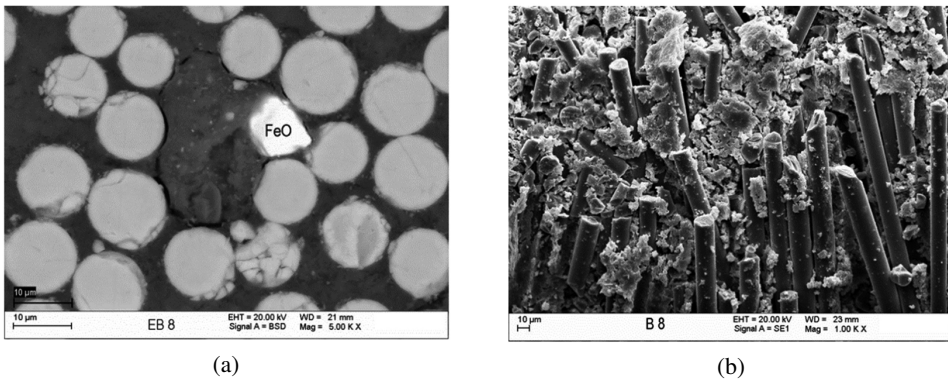


Fig. 5. SEM micrography of BFRP bar: a) 5000 \times magnification, visible basalt roving fibers – very bright area indicates FeO content; b) 1000 \times magnification, fiber destruction in the form of bends with breakages in the middle of the span of the sample

A detailed examination of the surface of the basalt fiber destruction showed the presence of micro-buckling of individual fibers and bends which is a typical phenomenon during bar compression (Fig. 5b). This type of destruction usually leads to longitudinal splitting, which results in the rupture of the bar structure, preventing the achievement of higher stresses in the outermost fibers. The phase-to-phase and volume fraction of fibers also have a significant impact on the failure mode due to the compression.

Based on the SEM analyses, it is possible to determine the bar architecture that influences its properties. In addition, the area of compression failure has been determined. The stiffness of the rod and thus the compressive strength depends on the chemical composition and the diameter of the filament.

3.2. Compressive strength of BFRP bars

During the tests, the following issues of bars destruction were observed:

1. For specimens with an unbraced length less than 85 mm ($L_f < 10d_b$), the bars were damaged by crushing. Within this range, the loading was applied until the specimen was crushed, and then, the load decreased rapidly after the bar was damaged. For all

samples in this group, damage occurred in the central part of the unbraced length of the specimens (Fig. 6a).

2. The specimens with an unbraced length in the range from $10d_b$ to $14d_b$ were slightly buckled in the final loading phase and then individual fiber groups were split, which, in turn, led to loss of load capacity (Fig. 6b).
3. Specimens with the unbraced length greater than $14d_b$ were buckled and then, in the final phase, the bars lost their load capacity due to excessive buckling, partial breaking of some fibers and de-bonding (Fig. 6c).

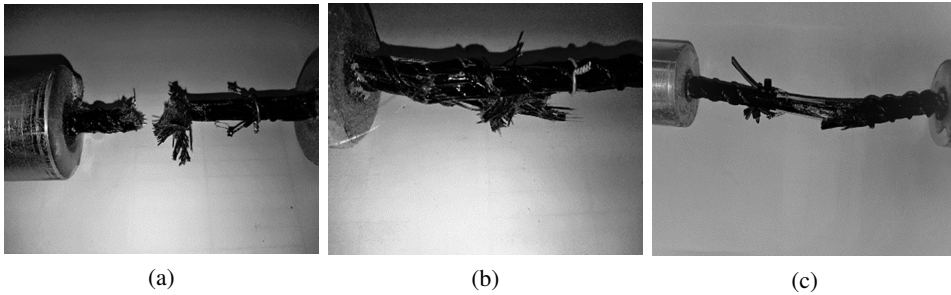


Fig. 6. Failure mode of BFRP bars: (a) crushing of the $6d_b$ free length specimen; (b) buckling with crushing the $12d_b$ free length specimen; (c) buckling of a $26d_b$ free length specimen

The average buckling load strength for samples with subsequent values of unbraced lengths, standard deviation and coefficient of variation are presented in Table 1. Column 1 shows the dimensionless proportionality coefficient of the free, unbraced length L_f related to the equivalent diameter of the bar d_b , in column 2 the unbraced length is expressed in millimetres. The buckling load strength $f_{f,c}$ was compared with the tensile strength

Table 1. Compression and tension characteristics of BFRP bars

L_f/d_b [-]	L_f [mm]	$f_{f,c}$ [MPa]	CoV [%]	$f_{f,c}/f_{f,t}$ [-]	$E_{f,c}$ [GPa]	$E_{f,c}/E_{f,t}$ [-]
4	35	356.94	5.48	0.32	41.58	0.95
6	50	375.71	6.32	0.34	41.79	0.95
10	85	475.43	4.27	0.43	49.87	1.14
12	100	429.57	2.83	0.39	42.61	0.97
14	120	375.71	4.65	0.34	43.69	1.00
16	140	278.11	7.81	0.25	56.27	1.28
20	170	184.26	5.32	0.17	45.16	1.03
22	185	182.47	9.27	0.17	50.45	1.15
26	220	143.95	9.86	0.13	51.69	1.18

$f_{f,t}$ and the modulus of elasticity under compression $E_{f,c}$ with the tension modulus of elasticity $E_{f,t}$ for BFRP bars with a nominal diameter of 8 mm supplied from the same batch of material.

The average tensile strength of BFRP bars with the same nominal diameter of 8 mm and the tensile modulus were $f_{f,t} = 1103.33$ MPa and $E_{f,t} = 43.87$ GPa, respectively (source: own research).

In the group of bars that were damaged due to crushing ($L_f < 10d_b$), the stress-strain relationships for different samples in the same group were linear and close to each other (Fig. 7a).

In the L_f range from $10d_b$ to $14d_b$, as the unbraced length increased, an increase in strain difference read from strain gauges located on opposite sides of the cross-section was observed. This phenomenon was associated with the observed method of failure consisting of crushing with slight buckling of bars (Fig. 7b).

For specimens with unbraced lengths $L_f > 14d_b$, the bars were significantly buckled. This phenomenon led to a reduction in the buckling load strength of the specimens as the unbraced length increased. Consequently, this resulted in a diametrical increase in readings on opposite strain gauges (Fig. 7c).

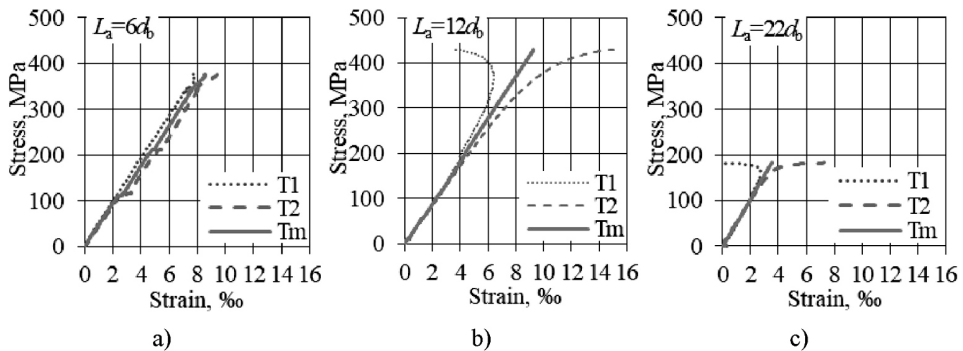


Fig. 7. Stress strain relationship a) free length $6d_b$, failure by crushing b), $12d_b$ free length, buckling with crushing; c) free length $22d_b$, buckling failure (T1, T2 strain gauges reading, Tm – average strain)

Due to the anisotropic structure of basalt fibers (known as a “weak anisotropy”), the modulus of elasticity under compression will be slightly different from the tension modulus of elasticity for BFRP bars. The values of the modulus of elasticity for subsequent unbraced lengths are shown in Table 1. Examples of stress – strain relationships for BFRP specimens are shown in Fig. 7.

3.3. The buckling load strength – unbraced length relationship

The dependencies of buckling load strength and the unbraced length of bars are presented in Fig. 8. During the tests, three mode of failure of BFRP bars were observed and distinguished, dividing its stress-unbraced length behaviour into three zones. The first mode

of failure consisted of crushing, which was observed in tests of specimens with an unbraced length of 35 to 85 mm (from $4d_b$ to $10d_b$). The bar was broken since the basalt fibers were separated from the epoxy matrix, with the individual fibers being split. In this area of occurrence of this type of failure (Fig. 8 zone 1), compressive strength is determined by the mutual influence of both anchored ends of the bar. An increase in compressive strength was observed with increasing of unbraced length of specimens. The relation in the crushing zone can be represented by the function of the second degree polynomial $f_{1,f,c}$.

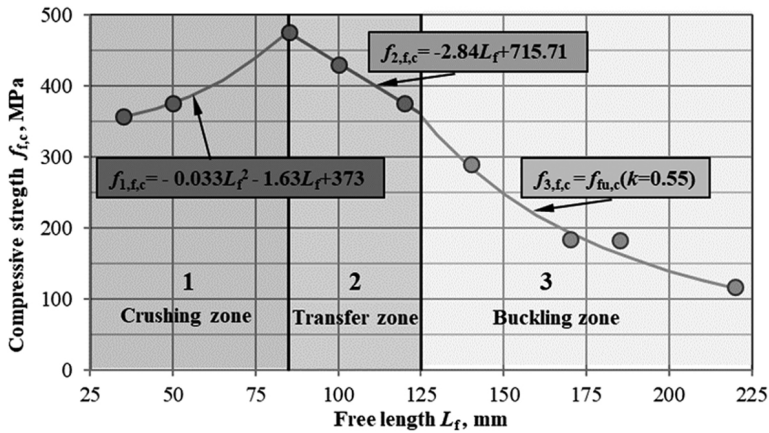


Fig. 8. Relationship buckling load strength – free unbraced length of a BFRP bar

The second mode of failure (zone 2 in the Fig. 8) is a combination of crushing and buckling. Samples with an unbraced lengths from 85 to 125 mm degraded first due to buckling, and after further loading, a failure occurred due to crushing. The buckling load strength in the “transient” area decreases with increasing of the unbraced length. The tendency to change buckling load strength in the transition zone can be represented by a linear function $f_{2,f,c}$ (Fig. 8).

The third failure mode consisted of gradual deepening of the bar buckling, as the load increased. In the final stage of loading, fiber breakage occurred in some specimens due to exceeding the value of ultimate stress in the middle section of the bar. The phenomenon of a “pure buckling” was recorded in samples with an unbraced length in the range from 125 to 220 mm. At the same time, it should be noted, that during buckling, the epoxy matrix and basalt fibers were connected (Fig. 5b). Nevertheless, even under ideal real conditions, the bars may have some manufacturing inaccuracies, while the load can be applied eccentrically or with offset distance. In this situation, the bent state exists practically from the very beginning of the deformation. However, its effect is small until the values of forces become critical.

Although the BFRP bars are not a completely homogeneous material, however, the Euler hyperbola with the coefficient $k = 0.55$ accurately maps the assessment of compressive strength in the general buckling zone. The proposed curve in buckling zone clearly approximates the values of compressive strength $f_{3,f,c} = f_{u,c}(k = 0.55)$ (Fig. 8).

4. Conclusions and recommendations

For BFRP bars with a nominal diameter of 8 mm, there is an optimal unbraced length $L_f = 85$ mm for which the ultimate buckling load strength reaches its maximum value while reaching the non-buckling condition.

Compressive strength, $f_{f,c}$, is dependent on unbraced length; its value is varying before reaching the optimal value (43% of tensile strength $f_{f,t}$) according to the polynomial curve for $L_f < 85$ mm, and then for the transition phase according to the linear relationship for $L_f < 125$ mm. In the last range, in the “pure buckling” phase for $L_f > 125$ mm it can be determined using the Euler curve with $k = 0.55$.

The strength of bar samples with an unbraced length of less than $10d_b$ (crushing zone) increased from 356.94 MPa to 375.71 MPa. Eventually, all specimens in this range of un-anchored length were crushed in the middle of the unbraced length.

The compressive strength of bars with unbraced length from $10d_b$ to $14d_b$ (transfer zone) decreased gradually along with the increase of the unbraced length from 475.43 MPa to 375.71 MPa. The samples slightly buckled in the final stage of loading, and then the individual groups of fibers split. This ultimately resulted in a loss of load-bearing capacity.

All samples of bars with an un-anchored length greater than $14d_b$ were buckling. Failure mode due to excessive buckling consisted in partial breaking of some fibers and defragmentation of individual filaments strands and their detachment. The compressive strength in the buckling zone decreased from 278.11 MPa to less than 144 MPa (for the largest tested unbraced length).

The values of the modulus of elasticity under compression, $E_{f,c}$, for non-buckled bars are similar to the modulus of elasticity under tension, $E_{f,t}$. For bars with larger unbraced lengths, the compressive modulus of elasticity was higher. With longer lengths of unbraced bars (buckling zone), buckling occurs in the bars under compression, which makes it impossible to reliably assess the modulus of elasticity. In composite materials, there is a change in the modulus of elasticity (not very large) with increasing stress. It should be noted that on the atomic scale, macroscopic elastic deformation manifests itself as slight changes in interatomic spacing and stretching of interatomic bonds. Consequently, the magnitude of the modulus of elasticity is a measure of the resistance to separation of adjacent atoms, i.e., the interatomic bond strength. The values of the modulus of elasticity for composite materials are lower compared to metals. These differences are a direct consequence of the different types of atomic bonds in the two types of materials.

Authors suggest that BFRP bars can be used as the compressive reinforcement after comprehensive examination of several influencing factors. The following conclusive remarks can be drawn:

- a) further research should be carried out to determine the relationship of the buckling load strength – unbraced length curves for the other diameters and types of FRP bars in order to propose a general relationship for the design of reinforcement in the compressed zone.
- b) factors that can influence the longitudinal buckling load strength of anisotropic bars include: epoxy matrix shear modulus, tensile modulus of elasticity, compressive

modulus of elasticity, fiber diameters, limit strains and matrix interfacial strength. In addition, misalignment of basalt fibers or their bending occurred during manufacturing process can reduce the longitudinal compressive strength of bars.

Acknowledgements

This work has been financially supported through the project no. PBS3/A2/20/2015 (2015–2018) “Innovative hybrid FRP rebar for infrastructure structures with high durability” granted by National Centre for Research and Development (NCBR).

References

- [1] M. Aslam, P. Shafigh, M.Z. Jumaat, S.N.R. Shah, “Strengthening of RC Beams Using Prestressed Fiber Reinforced Polymers – A Review”, *Construction and Building Materials*, 2015, vol. 82, pp. 235–256, DOI: [10.1016/j.conbuildmat.2015.02.051](https://doi.org/10.1016/j.conbuildmat.2015.02.051).
- [2] S.S. Zhang, T. Yu, G.M. Chen, “Reinforced Concrete Beams Strengthened in Flexure with Near-Surface Mounted (NSM) CFRP Strips: Current Status and Research Needs”, *Composites Part B: Engineering*, 2017, vol. 131, pp. 30–42, DOI: [10.1016/j.compositesb.2017.07.072](https://doi.org/10.1016/j.compositesb.2017.07.072).
- [3] K. Protchenko, E.D. Szmigiera, M. Urbański, A. Garbacz, “Development of Innovative HFRP Bars”, *MATEC Web of Conferences*, 2018, vol. 196, pp. 1–6, DOI: [10.1051/mateconf/201819604087](https://doi.org/10.1051/mateconf/201819604087).
- [4] N. Țăranu, G. Opreșan, D. Isopescu, I. Ențuc, V. Munteanu, C. Banu, “Fibre Reinforced Polymer Composites as Internal and External Reinforcements for Building Elements”, *Buletinul Institutului Politehnic Din Iași*, 2008, vol. 54, no. 1, pp. 7–20.
- [5] R. Kotynia, *FRP Composites for Flexural Strengthening of Concrete Structures Theory, Testing, Design*. Wydawnictwo Politechniki Łódzkiej, 2019.
- [6] K. Protchenko, M. Włodarczyk, E.D. Szmigiera, “Investigation of Behavior of Reinforced Concrete Elements Strengthened with FRP”, *Procedia Engineering*, 2015, vol. 111, pp. 679–686, DOI: [10.1016/j.proeng.2015.07.132](https://doi.org/10.1016/j.proeng.2015.07.132).
- [7] A. Garbacz, E.D. Szmigiera, K. Protchenko, M. Urbański, “On Mechanical Characteristics of HFRP Bars with Various Types of Hybridization”, in M. M. Reda Taha, U. Girum, & G. Moneeb, M. M. Reda Taha, U. Girum, & G. Moneeb (Eds.), *International Congress on Polymers in Concrete (ICPIC 2018): Polymers for Resilient and Sustainable Concrete Infrastructure*. Washington: Springer, 2018, pp. 653–658, DOI: [10.1007/978-3-319-78175-4_83](https://doi.org/10.1007/978-3-319-78175-4_83).
- [8] R.V. Balendran, T.M. Rana, T. Maqsood, W.C. Tang, “Application of FRP Bars as Reinforcement in Civil Engineering Structures”, *Structural Survey*, 2002, vol. 20, no. 2, pp. 62–72, DOI: [10.1108/02630800210433837](https://doi.org/10.1108/02630800210433837).
- [9] L.C. Hollaway, *Polymer Composites for Civil and Structural Engineering*. Blackie Academic and Professional Glasgow, 1993, pp. 12–62.
- [10] K. Protchenko, J. Dobosz, M. Urbański, A. Garbacz, “Wpływ Substytucji Włókien Bazaltowych przez Włókna Węglowe na Właściwości Mechaniczne Prętów B/CFRP (HFRP)”, *Czasopismo Inżynierii Lądowej, Środowiska i Architektury, JCEEA*, 2016, vol. 63, no. 1/1, pp. 149–156.
- [11] *Eurocode 2: Design of Concrete Structures – Part 1–1: General Rules and Rules for Buildings*. 2008.
- [12] *ACI 318-19 Building Code Requirements for Structural Concrete*. Detroit, Michigan: ACI Committee 318, 2019.
- [13] *ACI 440.1R-06 Guide for the Design and Construction of Structural Concrete Reinforced with FRP Bars*. American Concrete Institute: Detroit, Michigan, 2006.
- [14] *ACI 440.1R-15 Guide for the Design and Construction of Structural Concrete Reinforced with FRP Bars*. American Concrete Institute: Detroit, Michigan, 2015.

- [15] *CNR-DT 203 Guide for the Design and Construction of Concrete Structures Reinforced with Fiber Reinforced Polymer Bar*. Rome, Italy: National Research Council, 2006.
- [16] *Canadian Standards Association CAN/CSA S806-12 Design and Construction of Building Components with Fiber Reinforced Polymers*. Toronto: Rexdale, 2012.
- [17] M. Urbanski, A. Łapko, A. Garbacz, "Investigation on Concrete Beams Reinforced with Basalt Rebars as an Effective Alternative of Conventional R/C Structures", *Procedia Engineering*, 2013, vol. 57, pp. 1183-1191, DOI: [10.1016/j.proeng.2013.04.149](https://doi.org/10.1016/j.proeng.2013.04.149).
- [18] J. Sim, C. Park, D. Moon, "Characteristics of basalt fiber as a strengthening material for concrete structures", *Composites Part B- Engineering*, 2005, vol. 36, no. 6-7, pp. 504-512, DOI: [10.1016/j.compositesb.2005.02.002](https://doi.org/10.1016/j.compositesb.2005.02.002).
- [19] H. Zhu, G. Wu, L. Zhang, J. Zhang, D. Hui, "Experimental Study on the Fire Resistance of RC Beams Strengthened with Near-Surface-Mounted High-Tg BFRP Bars", *Composites Part B: Engineering*, 2014, vol. 60, pp. 680-687, DOI: [10.1016/j.compositesb.2014.01.011](https://doi.org/10.1016/j.compositesb.2014.01.011).
- [20] "Kamenny Vek". [Online]. Available: <https://basfiber.com/products>. [Accessed: 15.02.2020].
- [21] B.W. Rosen, "Mechanics of Composite Strengthening, Fiber Composite Materials", *American Society for Metals, Metals Park, Ohio*, 1965, vol. 37, pp. 37-75.
- [22] C.R. Schultheisz, A.M. Waas, "Compressive Failure of Composites, Part I: Testing and micromechanical theories", *Progress in Aerospace Sciences*, 1996, vol. 32, no. 1, pp. 1-42, DOI: [10.1016/0376-0421\(94\)00002-3](https://doi.org/10.1016/0376-0421(94)00002-3).
- [23] N.A. Fleck, B. Budiansky, "Compressive Failure of Fibre Composites Due to Microbuckling", in: *Inelastic Deformation of Composite Materials. International Union of Theoretical and Applied Mechanics, G.J. Dvorak, Ed.* New York: Springer, 1991.
- [24] P.K. Mallick, *Fiber Reinforced Composites, Materials, Manufacturing, and Design*. CRC Press, Taylor & Francis Group, 2008.
- [25] J. Militky, V. Kovacic, "Ultimate Mechanical Properties of Basalt Filaments", *Textile Research Journal*, 1996, vol. 66, no. 4, pp. 225-229, DOI: [10.1177/004051759606600407](https://doi.org/10.1177/004051759606600407).
- [26] W. Mingchao, Z. Zuoguang, L. Yubin, L. Min, S. Zhijie, "Chemical Durability and Mechanical Properties of Alkali-Proof Basalt Fiber and its Reinforced Epoxy Composites", *Journal of Reinforced Plastics and Composites*, 2008, vol. 27, no. 4, pp. 393-407, DOI: [10.1177/0731684407084119](https://doi.org/10.1177/0731684407084119).
- [27] A. Garbacz, E.D. Szmigiera, K. Protchenko, M. Urbański, "On Mechanical Characteristics of HFRP Bars with Various Types of Hybridization", in *International Congress on Polymers in Concrete (ICPIC 2018): Polymers for Resilient and Sustainable Concrete Infrastructure*, M.M. Reda Taha, Eds. Washington: Springer, 2018, pp. 653-658, DOI: [10.1007/978-3-319-78175-4_83](https://doi.org/10.1007/978-3-319-78175-4_83).
- [28] A. Garbacz, M. Urbański, A. Łapko, "BFRP Bars as an Alternative Reinforcement of Concrete Structures – Compatibility and Adhesion Issues", *Advanced Materials Research*, 2015, vol. 1129, pp. 233-241, DOI: [10.4028/www.scientific.net/AMR.1129.233](https://doi.org/10.4028/www.scientific.net/AMR.1129.233).
- [29] *ACI440.3R-12. Guide Test Methods for Fiber-Reinforced Polymers (FRPs) for Reinforcing or Strengthening Concrete Structures*. Farmington Hills, MI, USA: ACI, 2012.

Właściwości ściskanych prętów BFRP

Słowa kluczowe: zbrojenie BFRP, analiza SEM, elementy ściskane, ściskanie, wyboczenie, zgniatanie

Streszczenie:

Obecnie niezwykle dynamicznie rozwija się zastosowanie materiałów kompozytowych o wysokich parametrach użytkowych takich jak pręty BFRP (Basalt Fiber Reinforced Polymers) jako zamiennika tradycyjnego zbrojenia stalowego w budownictwie. W artykule przedstawiono ocenę wytrzymałości na obciążenie wyboczeniowe prętów BFRP, co umożliwi ich wykorzystanie, jako

zbrojenia w betonowych elementach ściskanych (słupy) oraz w strefie ściskanej elementów zginanych (np. belki i płyty).

W porównaniu ze zbrojeniem stalowym, pręty BFRP mają kilka istotnych zalet. Są to między innymi mały ciężar, wysoka wytrzymałość na rozciąganie, odporność na korozję, przezroczystość na pola magnetyczne. Natomiast w porównaniu do najbardziej rozpowszechnionych prętów GFRP (Glass Fiber Reinforced Polymers) wykazują zdecydowanie większą odporność na alkalia i kwasy. Włókna bazaltowe nie reagują toksycznie z powietrzem, wodą ani innymi chemikaliami, które mogą być niebezpieczne dla ludzi lub mogą zanieczyścić środowisko. Ponadto włókna bazaltowe nie są rakotwórcze. W trakcie recyklingu włókna przekształcają się w czarny proszek, który można łatwo usunąć z komory spalania i można go wykorzystać jako wypełniacz do różnych zastosowań.

Przeprowadzono jakościową i ilościową analizy składu pierwiastkowego przy użyciu spektrometru dyspersji energii wtórnego promieniowania X (EDS) które dostarczyły istotne informacje dotyczące składu prętów BFRP. We włóknach bazaltowych stwierdzono, obecność dominujących związków SiO_2 i Al_2O_3 , które występują także we włóknach szklanych. Ponadto odnotowano obecność związków żelaza Fe_2O_3 i FeO mających wpływ na fizyko-mechaniczne właściwości włókien bazaltowych, takich jak gęstość ($2,73 \text{ g/cm}^3$ dla włókien bazaltowych, w porównaniu do $2,54 \text{ g/cm}^3$ dla włókien szklanych typu E), kolor (od brązowego do matowo zielonego, w zależności od zawartości FeO), a także mniejsze przewodnictwo cieplne i lepszą stabilność temperaturową w porównaniu z włóknami szklanymi. Ustalono w badaniu metodą BSE konfigurację oraz niewielki rozrzut w średnicach włókien bazaltowych wchodzących w skład pręta BFRP.

Zachowanie prętów BFRP podczas ściskania dotychczas nie zostało określone. W programie badawczym zbadano 45 próbek BFRP o nominalnej średnicy 8 mm ze względu na ściskanie o zróżnicowanej długości niezakotwionej. Dla próbek o długości niezakotwionej do 85 mm zniszczenie następowało przez zginięcie. Pręty o długości niezakotwionej większej od 120 mm ulegały zniszczeniu w wyniku globalnego wyboczenia pręta a następnie pęknięcia włókien. Na podstawie zależności wytrzymałość na obciążenie wyboczeniowe – niezakotwiona długość pręta ustalono optymalną długość niezakotwioną pręta BFRP, dla której wytrzymałość na obciążenie wyboczeniowe osiąga największą wartość. Wraz ze wzrostem długości niezakotwionej wytrzymałość na obciążenie wyboczeniowe ulegała zmniejszeniu. Moduł sprężystości przy ściskaniu dla zmiennych długości niezakotwionych próbek nieznacznie się różnił, a jego wartość zbliżona była do modułu sprężystości przy rozciąganiu. Określono zależność między wytrzymałością na obciążenie wyboczeniowe a długością niezakotwioną prętów BFRP, co przyczyni się do optymalizacji rozstawu zbrojenia poprzecznego w elementach ściskanych oraz do opracowania przepisów normowych w obszarze elementów ze zbrojeniem ściskany.

Received: 30.11.2021, Revised: 08.02.2022